Microchemical Journal 154 (2020) 104531

Contents lists available at ScienceDirect

Microchemical Journal

journal homepage: www.elsevier.com/locate/microc

Determining the provenance of the European glass beads of Lumbu (Mbanza Kongo, Angola)

Mafalda Costa[a,b], Pedro Barrulas[a], Luís Dias[a], Maria da Conceição Lopes[c,d], João Barreira[c], Bernard Clist[e,f], Karlis Karklins[g], Maria da Piedade de Jesus[h], Sónia da Silva Domingos[i], Luc Moens[j], Peter Vandenabeele[b,j], José Mirão[a,k,*]

[a] HERCULES Laboratory, University of Évora, Palácio do Vimioso, Largo Marquês de Marialva 8, 7000-554 Évora, Portugal
[b] Archaeometry Research Group, Department of Archaeology, Ghent University, Sint-Pietersnieuwstraat 35, B-9000 Ghent, Belgium
[c] Research Center in Archaeology, Arts and Heritage Sciences, University of Coimbra, Palácio de Sub-Ripas, 3000-395 Coimbra, Portugal
[d] Department of History, Archaeology and Arts, Faculty of Arts and Humanities, University of Coimbra, Largo da Porta Férrea, 3004-530 Coimbra, Portugal
[e] Department of Languages and Cultures, BantUGent – UGent Centre for Bantu Studies, Ghent University, Blandijnberg 2, 9000 Ghent, Belgium
[f] Institut des Mondes Africains (IMAF), Paris, France
[g] Society of Bead Researchers, Ottawa, Ontario, Canada
[h] Instituto Nacional do Património Cultural (INPC), Rua Major Kanhangulo 77/79, CP1267, Luanda, Angola
[i] Centro Nacional de Investigação Científica (CNIC), Avenida Ho Chin Min 201, CP34 Mainanda, Luanda, Angola
[j] Raman Spectroscopy Research Group, Department of Chemistry, Ghent University, S-12, Krijgslaan 281, B-9000 Ghent, Belgium
[k] Department of Geosciences, School of Science and Technology, University of Évora, Colégio Luís António Verney, R. Romão Ramalho, 59, 7000-671 Évora, Portugal

ARTICLE INFO

Keywords:
Sourcing
LA-ICP-MS
European trade beads
Mbanza Kongo
Kongo Kingdom

ABSTRACT

A collection of glass beads found in Lumbu (Mbanza Kongo, Angola) were analyzed by means of a multi-analytical minimally invasive methodology, which included handheld X-ray fluorescence (hXRF), variable pressure scanning electron microscope coupled with energy dispersive X-ray spectrometry (VP-SEM-EDS), micro-Raman spectroscopy and laser ablation inductively coupled plasma mass spectrometry (LA-ICP-MS).

Trace element analysis, and rare earth element pattern analysis in particular, was found to be essential to establish the provenance of the European trade beads in this study. The glass beads from types 30, 31, 32, 36, 38, 39, 40, 41, 42, 43 and 45 were found to have been produced in Venice, and the glass beads from types 26 and 28 have been assigned to the Bohemian glass industry.

While determining the provenance of each glass artefact was a major goal of this study, the process of glass coloring and opacification was also studied in an attempt to establish the technology employed in the production of these artefacts. Chemical data indicate that cobalt and copper were used to produce blue hues, while a combination of copper and iron ions was used to produce green glass. Black colored glass was obtained by the combined use of iron and manganese ions, whereas the iron-sulfur chromophore was used to impart a distinct amber hue to the glass. Red was produced using trace amounts of metallic gold particles (ruby red glass) and metallic copper nano-particles or cuprous oxide (brownish-red glass). Lead arsenates, calcium phosphate, and cassiterite were used as opacifying agents.

The use of both morphological and chemical analysis enabled the identification of distinct European production centers, allowing a glimpse into the consumption patterns and economic interactions in place between Europe and West-Central Africa throughout the 17th-19th centuries.

1. Introduction

Man-made glass artefacts are some of the most common materials found in archeological contexts. First developed in western Asia in the 3rd millennium B.C., glass composition has changed throughout time. While silicate glass remained the most prevalent glass from ancient to historic times, the fluxing agents, glass stabilizers and (de)coloring agents used in glass manufacture changed according to raw material availability and fashion and market preference or technological knowledge.

* Corresponding author at: HERCULES Laboratory, University of Évora, Largo Marquês de Marialva 8, 7000-809 Évora, Portugal.
E-mail addresses: mcosta@uevora.pt, peter.vandenabeele@ugent.be (M. Costa), pbarrulas@uevora.pt (P. Barrulas), luisdias@uevora.pt (L. Dias), conlopes@ci.uc.pt (M.d.C. Lopes), bernardolivier.clist@ugent.be (B. Clist), luc.moens@ugent.be (L. Moens), jmirao@uevora.pt (J. Mirão).

https://doi.org/10.1016/j.microc.2019.104531
Received 30 August 2019; Received in revised form 10 December 2019; Accepted 10 December 2019
Available online 16 December 2019
0026-265X/

In order to produce silicate glass, sand or other silica sources, such as crushed quartz pebbles, were mixed with alkaline or alkaline-earth oxides, known as glass modifiers or fluxing agents. The cations of the fluxing agents create a weakness in the structure and lower its melting temperature [1,2]. After the fall of the Roman Empire, in Europe, plant ash was used to substitute the most common mineral fluxing agent – natron. The composition of plant ash is variable and depends on the plant species chosen, the composition of the soil, ground water and overall environment where they grew, the plant's growing stage, the part of the plant that was ashed (leaves versus woody components), and even the burning process [3,4]. Halophytic plant ashes, rich in soda and known as *allume catina* in the Venetian glass industry, were first imported from the Levantine coast in the 13th century [2,5]. A lower quality soda plant ash, known as *barilla* was produced in Europe by burning local plants in the 17th century onwards in Italy and Spain [2]. According to contemporaneous treaties, purification methods were first introduced in the 15th century in order to obtain purer plant ashes, free of non-soluble components [2]. Wood ash, on the other hand, was first introduced in Europe in 800 A.D. [5]. This plant ash, produced by burning forest plants, is rich in potassium and was exclusively used in the production of the Central and Western European glass known as forest glass or *Waldglas* [5,6]. *Gripola di vino*, tartar from wine barrels, was used in the Venetian glass industry as their main potash source [2]. The combined use of *allume catina* and *gripola di vino* is mentioned in the 1536 anonymous manuscript of Montpellier which describes several glass recipes [2].

Alumina and alkaline-earth ions (generally Ca^{2+} and Mg^{2+}) act as glass stabilizers, counteracting the structural weakness introduced by the fluxing agents and creating a more stable and durable glass, capable of better withstanding water damage and surface decay [1,2]. Glass stabilizers can be introduced deliberately or as impurities present within the sand in the form of feldspars, clays and calcite/aragonite (limestone or shell fragments). High amounts of calcium and magnesium can also be found in plant ash [4]. Lead oxides can also be used as glass stabilizers. Lead oxides have been used in glass production in Europe since the Iron Age [3], but the Venetian glass industry diffused and rebranded glass containing these compounds as *vetro di piombo* [2]. In reality, lead oxides can have a triple function, behaving as glass formers (partially or totally substituting silica), fluxing agents and glass stabilizers.

Glass color is linked to the presence of small amounts of transition metal ions or metallic particles within the glass structure and known as (de)coloring agents. The transition metal ions' oxidation state, along with their position in the glass network are two of the main characteristics responsible for the final color obtained [7]. The opacity of a glass is also dependent on the particles dispersed within the glass matrix [1,8].

Hence, glass composition is dependent on the raw materials used (and their purity) and the melting conditions present at the time of manufacture.

1.1. Glass provenance

Determining the provenance of glass artefacts has been the subject of many studies (e.g.[9–24].). Geochemical studies, in particular, have the potential to link glass artefacts to the geological source of the raw materials used in their production due to their unique fingerprint [13]. This means the term *provenance* refers not to the actual location of glass production, but to the geographical location from which the raw materials were recovered. While fluxing agents and (de)colorants are commonly traded between different communities, favored silica sources used in glass production are usually fairly local [25–27]. Silica sources deemed suitable for glass production are chosen based on their purity and particle size. The purity of a silica source depends on its origin and the type of rock from which it derives. Sand maturity is also dependent on transportation distance before deposition. Mature sediments are not only more uniform in appearance, with similar particle size and significant roundness, but are also composed primarily of very resistant and stable minerals such as quartz and zircon ($ZrSiO_4$). However, the sands used in glass production generally contain minor amounts of additional minerals such as mica, clays, feldspars, and other aluminosilicates, rare earth element (REE) phosphates (e.g. monazite and xenotime), chromite ($FeCr_2O_4$), and iron and/or titanium oxides (e.g. magnetite, ilmenite and rutile) [24,28,29]. The presence of these non-quartz minerals within the silica source used in glass manufacture will be reflected in the composition of the glass artefacts produced. Trace elements such as Sc, Ti, V, Cr, Fe, Co, Ni and Nb can be found in iron-titanium oxides, while Zr and Hf are associated with zircon [24,29]. Ba and Rb can be present in K-bearing minerals such as clay-minerals or K-feldspars, while Sr commonly substitutes Ca in plagioclases and other Ca-containing minerals [29]. REE and Y are concentrated in the clay fraction of sands, but also in heavy minerals such as monazite and other REE phosphates, all well as zircon [13,29].

Studies have shown that the largest portion of REE found in glass can be attributed to the silica source, as these elements occur in insignificant concentrations in both plant ash and carbonates [24]. REE concentrations are also not influenced by the use of (de)colorants [14]. While other trace elements can be influenced by erosion and sedimentation processes, REE preserve the signature of the source rock [22]. Moreover, the behavior of europium (Eu) and cerium (Ce) in relation to the other REE reflect the redox conditions of the chemical system in which REE-containing minerals were formed. The fractionation of Eu and Ce relative to neighboring trivalent rare earth elements is known as europium and cerium anomaly, respectively [18,28]. Europium anomalies are a product of igneous processes such as plagioclase formation [22], while cerium fractionation can occur in marine environments during processes of cementation, lithification and precipitation [28]. Besides the use of REE patterns (e.g. [9,11–14,16–18,22–24]), Zr-Ti [10], Zr-Ti-Cr-La [19] and Zr-Sr-Ba [21] have been used to successfully distinguish between different silica sources.

1.2. Glass sourcing in sub-Saharan Africa

Glass beads have been found in many archeological sites in sub-Saharan Africa dated to the last 2000–3000 years [17]. These artefacts are usually testaments of trade networks between sub-Saharan African societies and glass working communities located in North Africa and Eurasia [23]. In African societies, glass beads were commonly used as adornments or amulets to symbolize wealth, social status and political, cultural and religious affiliation [30]. These objects were also used as currency [31].

Despite the increasing number of glass bead assemblages found in sub-Saharan Africa, studies with trace element analysis are rare. In fact, most works focus on glass beads from the Islamic mercantile network or the Indian Ocean trade [9,12,17,18,20,23,32–34], with barely any studies regarding European trade beads [15,16,35]. Koleini et al. recently authored a general overview of all glass beads found in Sub-Saharan Africa that have been subjected to archaeometric studies [36].

2. Materials & methods

2.1. Materials

Located in Mbanza Kongo, the capital of the Kongo Kingdom [37,38], Lumbu is thought to be either the site of the Royal palace [39], or an area used by the King to hold public audiences when important state matters were being decided [40]. The archeological excavations carried out in 2014 by S. da Silva Domingos (CNIC, Angola), and Christophe Mbida and Raymond Assombang (University of Yaoundé I, Cameroon), uncovered a collection of 52 glass beads along with an assortment of locally produced and Portuguese pottery and clay pipe

Table 1
Isotopes analyzed by LA-ICP-MS and their respective dwell times.

Dwell time (ms)	Isotope
5	^{23}Na; ^{27}Al; ^{28}Si; ^{39}K; ^{44}Ca; ^{56}Fe
10	^{11}B; ^{24}Mg; ^{47}Ti; ^{52}Cr; ^{55}Mn; ^{57}Fe; ^{59}Co; ^{60}Ni; ^{63}Cu; ^{66}Zn; ^{67}Zn; ^{75}As; ^{85}Rb; ^{88}Sr; ^{89}Y; ^{90}Zr; ^{118}Sn; ^{121}Sb; ^{208}Pb
20	^{31}P; ^{45}Sc; ^{51}V; ^{93}Nb; ^{107}Ag; ^{133}Cs; ^{137}Ba; ^{139}La; ^{140}Ce; ^{141}Pr; ^{146}Nd; ^{147}Sm; ^{153}Eu; ^{157}Gd; ^{159}Tb; ^{163}Dy; ^{165}Ho; ^{166}Er; ^{169}Tm; ^{172}Yb; ^{175}Lu; ^{178}Hf; ^{181}Ta; ^{197}Au; ^{209}Bi; ^{232}Th; ^{238}U

fragments.

A total of 21 glass beads were analyzed in this study. The glass beads were initially separated based on morphological characteristics into typological groups. A detailed description of each typological group including color, size, manufacturing technique and probable origin and production date (when known), can be found in Table S1 (Supplementary information).

2.2. Methods

The methodology used in this study follows the one proposed by Costa et al. [16].

2.2.1. Handheld X-ray fluorescence (h-XRF)

Handheld XRF measurements were acquired in-situ in Mbanza Kongo (Angola) using a Bruker™ Tracer III SD® XRF with a silicon-drift XFlash ® detector (SDD) and a Rh-target delivering a polychromatic X-ray beam of 3 × 3 mm. Spectra were recorded in vacuum conditions during a 120-s real-time count, using a voltage of 40 kV and a current intensity of 35 μA. All spectra were recorded using the S1PXRF software (Bruker™) and processed using the Artax (Bruker™) software in order to obtain semi-quantitative data.

Each sample was analyzed in one or more locations according to their size and color – mono-colored vs. multi-colored. The generated net areas of the fluorescence lines were normalized to the counts of the Rh Kα lines [16,41].

Only a limited amount of samples could be transported to Europe for further analysis. Therefore, the use of hXRF was essential to identify and discriminate compositional groups and select the beads to be analyzed by VP-SEM-EDS, LA-ICP-MS and micro-Raman spectroscopy.

2.2.2. Variable pressure scanning electron microscope coupled with energy dispersive X-ray spectrometry (VP-SEM-EDS)

VP-SEM-EDS was performed using a Hitachi™ S3700N SEM coupled to a QUANTAX EDS microanalysis system equipped with a Bruker™ XFlash 5010 SDD EDS Detector® with 129 eV spectral resolution at FWHM/Mn Kα. The samples were analyzed at low vacuum (40 Pa) and with an accelerating voltage of 20 kV and a 10–12 mm working distance. The variable pressure approach allows imaging and chemical analysis without the need of coating. The SEM images were acquired in the backscattering mode. The EDS data was processed in the Espirit1.9 software using the standardless tools [16,41,42].

2.2.3. Micro-Raman spectroscopy

A Bruker™ Optics SENTERRA dispersive Raman spectrometer coupled with a BX51 Olympus™ microscope was used to record the Raman spectra. The system uses a thermo-electrically cooled CCD detector, operating at −65 °C. At least three spectra per sample were acquired using a Nd:YAG laser (532 nm) at high resolution (3–5 cm^{-1}) and in the range of 60–2750 cm^{-1}. The 20 × objective was used for all the samples, with a spot size of approximately 10 μm. The measuring time, laser power, and number of accumulations were set to obtain a good signal-to-noise ratio using the Bruker™ OPUS software.

The collected Raman spectra were further processed using the GRAMS software (ThermoFisher Scientific™). Following previous authors (e.g. [16,42–45]), a 4-segment linear baseline was subtracted using fixed points at approximately 200, 700, 800 and 1200 cm^{-1} to characterize the glass matrix. The glass massifs were subsequently subjected to curve fitting in order to allow for reproducible results and for comparison with published data.

2.2.4. Laser ablation inductively coupled plasma mass spectrometry (LA-ICP-MS)

LA-ICP-MS analyses were conducted using a CETAC LSX-213 G2+ laser ablation system coupled to an Agilent™ 8800 Triple Quad ICP-MS. The glass beads were mounted on the ablation cell without any previous sample preparation. A 100 μm spot size with a frequency of 20 Hz and a laser output energy of 80% (3 mJ/pulse at 100%) was used to analyze 4–12 spots in glass beads (4 distinct locations were analyzed in each color in the case of multi-colored beads). Each spot had a total acquisition time of 75 s, including a 10 s washout. Helium, with a flow of 1 L/min, was used as a carrier gas in the LA system and the ICP-MS data was acquired in MS/MS mode. The NIST 612 glass standard was used for the calibration of the ICP-MS prior the analysis. Fractionation and oxide formation were monitored using the ^{238}U/^{232}Th ratio and the ^{248}ThO/^{232}Th ratio, respectively. The NIST 612 glass standard was analyzed at the beginning and end of each sequence and at 20–24 spot intervals for drift determination and correction if needed. The isotopes that were analyzed and their respective dwell times can be found in Table 1. Data of two different Fe and Zn isotopes were acquired and used to determine possible instrumental interferences. Elemental concentrations were determined using off-line calculations and data reduction with the GLITTER® software, using NIST 612 as primary reference material (recommended concentrations reported by Pearce et al. [46]) and SiO_2 as an internal standard for the samples and reference material. The first 4 or 5 s of ablation were discarded to eliminate the interference of surface contamination and weathering.

3. Results & discussions

3.1. Chemical glass types

VP-SEM-EDS results displayed in Table 2 revealed that several glass bead types have significant lead content. In fact, according to the glass type classification devised by Schalm et al. [47], the white and red glass of the type 36 beads can be classified as lead glass (PbO > 15 wt.%). However, as previously mentioned, lead can assume different roles within a glass; it can act as a glass former, fluxing agent and glass stabilizer, but it can also interact with other elements present in the glass melt, causing the precipitation of crystals that influence both color and transparency [2]. Caution must be exercised when classifying artefacts as being composed of lead glass, as understanding the behavior assumed by this element is essential to correctly define glass type. This aspect will be further discussed in the following sections.

A comparison between the Na_2O and K_2O concentrations determined by VP-SEM-EDS and LA-ICP-MS (Table 3) revealed that an important number of glass beads have suffered processes of glass alteration. Glass alteration is controlled by the pH of the burial environment and can be described by two reaction processes: selective leaching and uniform dissolution [48,49]. In selective leaching water reacts with the glass removing alkali ions (Na^+ and K^+) and transition metal cations, resulting in dealkalinized silica-rich glass. The results

Table 2
Chemical analyses (oxides wt.%) obtained by VP-SEM-EDS.

	26	28	30	31	32	33	36W	36R	38W	38G	38R	39	40	41	42	43	45
Na_2O	8.0	4.2	9.7	2.9	13.3	7.9	1.1	1.6	9.9	11.1	14.0	7.1	4.5	3.1	5.6	3.2	3.1
MgO	0.4	0.8	2.5	1.2	4.4	0.2	n.d.	n.d.	3.7	3.5	5.0	1.0	1.9	2.6	2.2	1.3	3.4
Al_2O_3	1.9	1.9	2.8	9.3	3.2	7.4	3.7	14.1	5.0	3.6	4.0	8.3	7.9	3.1	4.7	8.4	4.1
SiO_2	65.4	65.7	69.0	66.5	57.7	61.8	4.9	29.2	44.2	56.8	47.7	74.7	63.3	76.0	65.1	70.5	79.2
P_2O_5	0.4	2.9	0.2	0.6	0.2	n.d.	13.9	9.0	1.1	0.8	1.0	n.d.	1.8	n.d.	0.7	1.2	n.d.
SO_2	0.4	0.5	0.3	0.2	0.7	n.d.	n.d.	n.d.	n.d.	0.6	n.d.	0.6	n.d.	0.6	0.4	n.d.	1.3
Cl	0.4	0.7	0.3	0.9	0.8	n.d.	1.7	1.5	n.d.	0.9	1.0	0.6	0.8	0.7	0.9	1.0	1.6
K_2O	6.4	13.5	3.1	4.4	3.2	5.4	0.6	2.3	2.2	3.7	3.2	3.9	4.6	2.5	2.9	4.1	0.9
CaO	11.5	8.9	8.6	7.0	11.8	6.8	11.1	7.3	8.4	13.0	9.6	1.9	7.5	7.7	12.7	7.0	5.3
TiO_2	n.d.	n.d.	n.d.	0.7	n.d.	n.d.	n.d.	1.2	n.d.	n.d.	n.d.	n.d.	0.3	n.d.	n.d.	0.3	n.d.
MnO	4.2	n.d.	n.d.	3.0	3.3	n.d.	n.d.	n.d.	n.d.	n.d.	0.7	n.d.	4.0	n.d.	n.d.	0.3	n.d.
FeO	0.5	n.d.	1.3	3.2	1.4	n.d.	1.9	4.8	2.1	3.9	5.0	1.3	2.5	1.0	3.7	2.6	1.1
CoO	0.4	0.9	n.d.	n.d.	n.d.	n.d.	n.d.	n.d.	n.d.	n.d.	n.d.	n.d.	n.d.	n.d.	n.d.	n.d.	n.d.
CuO	n.d.	n.d.	2.2	n.d.	n.d.	2.2	n.d.	n.d.	n.d.	2.1	1.0	n.d.	n.d.	2.8	1.2	n.d.	n.d.
SnO_2	n.d.	n.d.	n.d.	n.d.	n.d.	n.d.	n.d.	n.d.	9.2	n.d.	n.d.	n.d.	n.d.	n.d.	n.d.	n.d.	n.d.
As_2O_3	n.d.	n.d.	n.d.	n.d.	n.d.	n.d.	4.0	1.8	n.d.	n.d.	n.d.	n.d.	n.d.	n.d.	n.d.	n.d.	n.d.
PbO	n.d.	n.d.	n.d.	n.d.	n.d.	8.3	57.1	27.2	14.2	n.d.	7.8	n.d.	1.0	n.d.	n.d.	n.d.	n.d.

Table 3
Comparison between the Na_2O and K_2O concentrations determined by VP-SEM-EDS and LA-ICP-MS.

VP-SEM-EDS (wt.%)	26	28	30	31	32	33	36W	36R	38W	38G	38R	39	40	41	42	43	45
Na_2O	8.0	4.2	9.7	2.9	13.3	7.9	1.1	1.6	9.9	11.1	14.0	7.1	4.5	3.1	5.6	3.2	3.1
K_2O	6.4	13.5	3.1	4.4	3.2	5.4	0.6	2.3	2.2	3.7	3.2	3.9	4.6	2.5	2.9	4.1	0.9

LA-ICP-MS (wt.%)	26	28	30	31	32	33	36W	36R	38G	38W	38R	39	40	41	42	43	45
Na_2O	12.3	3.5	19.0	12.7	12.1	14.3	0.3	1.4	11.9	9.4	10.5	19.4	13.0	20.1	14.2	15.6	18.9
K_2O	6.0	12.8	3.3	5.6	2.5	4.7	0.8	6.6	2.4	1.8	2.1	2.5	2.7	2.1	2.3	2.6	2.7

shown in Table 3 highlight the surface-sensitive nature of SEM-EDS – a technique with an analysis depth of approximately 1–2 μm [50] – and the importance of discarding the first 4–5 s of ablation in LA-ICP-MS. The presence of a network of small cracks on the glass surface, often accompanied by glass detachment, are microscopic signs of glass decay which were found by VP-SEM (Fig. 1).

The ternary diagram of the normalized concentrations of Na_2O, MgO + K_2O and CaO (Fig. 2) has been used to define the main chemical glass types based on their alkali metal source (e.g. [51]). Fig. 2 shows that all the glass beads in this study fall into one of the following chemical glass types: soda-lime plant ash glass (II) or mixed alkali soda-potash glass (III) [51].

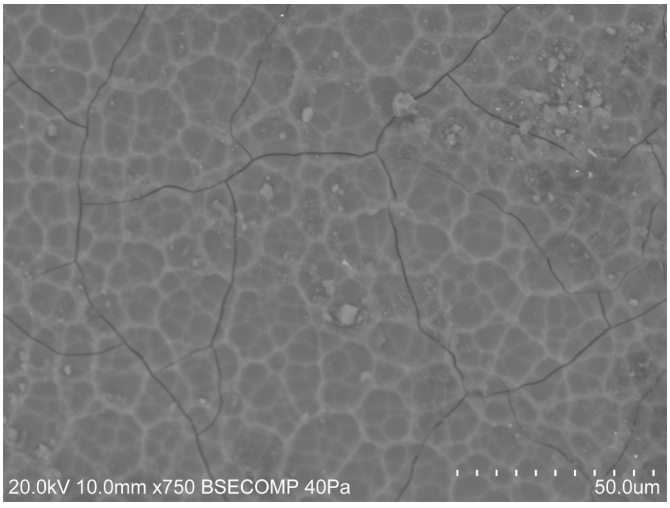

Fig. 1. VP-SEM image of a type 31 glass bead showing evidences of glass decay: presence of a network of small cracks on the glass surface.

The glass beads from types 31, 38 and 40 have been previously attributed to the Venetian glass industry (Table S1 – Supplementary information). As seen in Fig. 2, The glass beads from types 38 and 40 fall within the compositional window of plant ash soda-lime glass (group II). These results are consistent with the use of halophytic plant ashes, known as *allume catina*, as the main fluxing agent. As previously mentioned, *allume catina* was imported from the Levantine coast since the 13th century [2,5] and is commonly mentioned in Venetian treaties from the 16th and 17th centuries [2]. The glass beads from type 31, on the other hand, have an intermediate composition between groups II and III (Fig. 2), which could indicate that a lower quality soda plant ash, such as *barilla*, or the combined use of *allume catina* and *gripola di vino* may have been used to produce them. Previous studies of European trade beads found in Angola determined that halophytic plant ashes, as well as variable quality plant ash or a combination of *allume catina* and *gripola di vino* was employed in the 18th to early 20th century Venetian glass bead production [16].

Glass beads produced in Central Europe (Bohemia and Bavaria) and found in Angola were previously studied by Costa et al. [16]. Their results, which indicated that potash plant ash (or wood ash) was used to produce these glass beads [16], were consistent with what is known of the medieval and early modern Central European glass production (e.g. [6,52,53]). The use of potash in the Bohemian glass industry, in particular, is well known and described in literature (e.g. [6]). However, the glass beads from types 26 and 28, previously attributed to the Bohemian production (Table S1 – Supplementary information), did not fall within the of potash-lime plant ash compositional group (group IV; Fig. 2). Instead, the beads from type 26 can be classified as soda-lime glass (group II), while the glass beads from type 28 fall into the mixed alkali soda-potash compositional group (group III). Evidences of the use

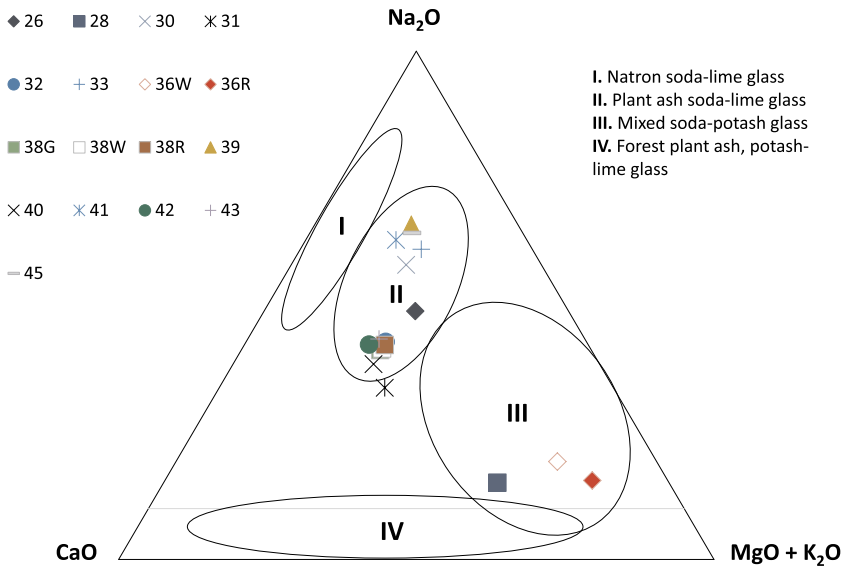

Fig. 2. Ternary diagram of the normalized Na2O, MgO + K2O and CaO contents of the glass beads analyzed by LA-ICP-MS. Four main chemical glass types are evidenced by the ellipses [51].

of different fluxing agents in the Bohemian glass industry have not been found in the literature. However, Cílová & Woitsch [6] mention that potash trade during the 17th to the 19th century expanded, and that Central European glass produced at the time was "often made of a mixture of materials (among them, potash) from different origins". Therefore, based merely on chemical glass type, a non-Bohemian origin for the glass beads of type 26 and 28 cannot be excluded.

As seen in Fig. 2, the glass beads of unknown origin (Table S1 – Supplementary information) fall into two categories: 1) the soda-lime glass compositional group (group II; types 30, 32, 33, 39, 41, 42, 43 and 45); 2) the mixed alkali soda-potash compositional group (group III; type 36). These results indicate that the glass beads from types 30, 32, 39, 41, 42, 43 and 45 were produced using halophytic plant ashes, whereas *barilla*, a lower quality soda plant ash, or the combined use of *allume catina* and *gripola di vino* may have been used to produce the 36 glass beads. While the composition of these glass beads could suggest a Venetian origin, it is important to note that although the Venetian recipes were considered to be a guild secret, a number of Venetian glassmakers opened their own glasshouses in Flanders and London [54], making it impossible to identify the production centers of these glasses based solely on their chemical glass type. Moreover, the reported mixing of fluxing agents used in Central Europe in the 17th-19th centuries hinders the determination of the manufacture region responsible for the production of the 36 glass beads.

3.2. Glass (de)colorants and opacifying agents

3.2.1. Blue glass beads (types 26, 28, 30, 32, 33, 41 and 43)

The blue glass beads found in Lumbu can be divided into two groups according to the main colorant responsible for their blue hue. Significant amounts of Co were by hXRF in the blue beads from types 26, 28, 32 and 43, while Cu was found to be responsible for the blue hues of the beads from types 30, 33 and 41 (Fig. 3a). Copper (Cu^{2+}) and cobalt (Co^{2+}) are among the most common coloring agents used in glass production [55]. In their divalent state, both of these transition metal ions impart blue hues to glass [56]; cobalt colored glass has a deep blue hue, whereas Cu^{2+} ions impart a turquoise color to glass. While the concentration in which these metallic ions are present will influence the final hue, it is important to note that Co^{2+} ions possess a high absorption coefficient, allowing small concentrations (CoO ~ 0.1%) to produce a distinct dark blue color [55]. In fact, as seen in Table 2, cobalt could not be detected by VP-SEM-EDS in the beads from types 32 and 43. This can be explained by the low detection limits of the instrument (~ 0.1% [57]). LA-ICP-MS revealed that the Co concentrations the blue beads from types 32 and 43 are approximately 689 ppm and 911 ppm, respectively.

Cobalt is generally exploited as a by-product of copper, nickel, silver, gold, lead or zinc extraction [58,59], but it can also be associated iron and/or arsenic minerals [59]. Determining the provenance of cobalt relies, therefore, on the minor and trace elements that are associated with this transition metal. Many studies have focused on determining the provenance of cobalt blue pigments used in glass and glaze production (e.g. [51,60–62]). However, the use of different analytical techniques and the small number of samples analyzed limits the development of a chronology of cobalt sources used throughout history. Moreover, many pigment sources remain unknown [51,61]. A careful examination of the hXRF and LA-ICP-MS results revealed that cobalt was associated with Ni, As and Zn in the blue glass beads from types 26, 28, 32 and 43 (Figures S1 and S2 – Supplementary information). Variable correlations between cobalt and Fe, Cr, Bi, Ag, U and Mn were also found (Figures S1 and S2 – Supplementary information). These results suggest that the cobalt used in the production of these blue glass beads came from the Erzgebirge mining district, one of the main Co sources used in the production of glasses and glazes [60]. Erzgebirge, a 150 km long mountain range located on the Germany-Czech Republic border, is part of the metamorphic basement of the internal Mid-European Variscides [63,64]. Its complex geology is characterized by granitic plutonism and medium-to high-grade metamorphism [63,65], which enabled the formation of granodioritic orthogneisses, phyllites, mica schists, eclogites and skarns [63,65,66]. The Erzgebirge mining region hosts both hydrothermal five-element Ni-Co-As-Ag-Bi(-U) veins and polymetallic sulfide veins [65,67,68]. Gangue minerals of five-element type deposits are mainly quartz and various carbonates [68]; the presence of both ankerite ($Ca(Fe^{2+},Mg)(CO_3)_2$) and rhodocrosite ($MnCO_3$) have been reported in the Schneeberg area (Germany) by Dayton [69], while Ondrus et al. [65] mentions calcite, manganoan calcite and dolomitic carbonate, accompanied by quartz, fluorite and barite in the Joachimsthal ore district (Czech Republic). Bastin [70] when describing the Erzgebirge mining district, states that the cobalt-silver veins occasionally combine with or grade into iron-manganese veins. The presence of iron-manganese veins, along with the Fe- and/or Mn-rich gangue can cause significant variability in the concentration of both these elements in the silver extraction Co-rich by-product used in the production of cobalt blue glass. The variable correlation of Co and

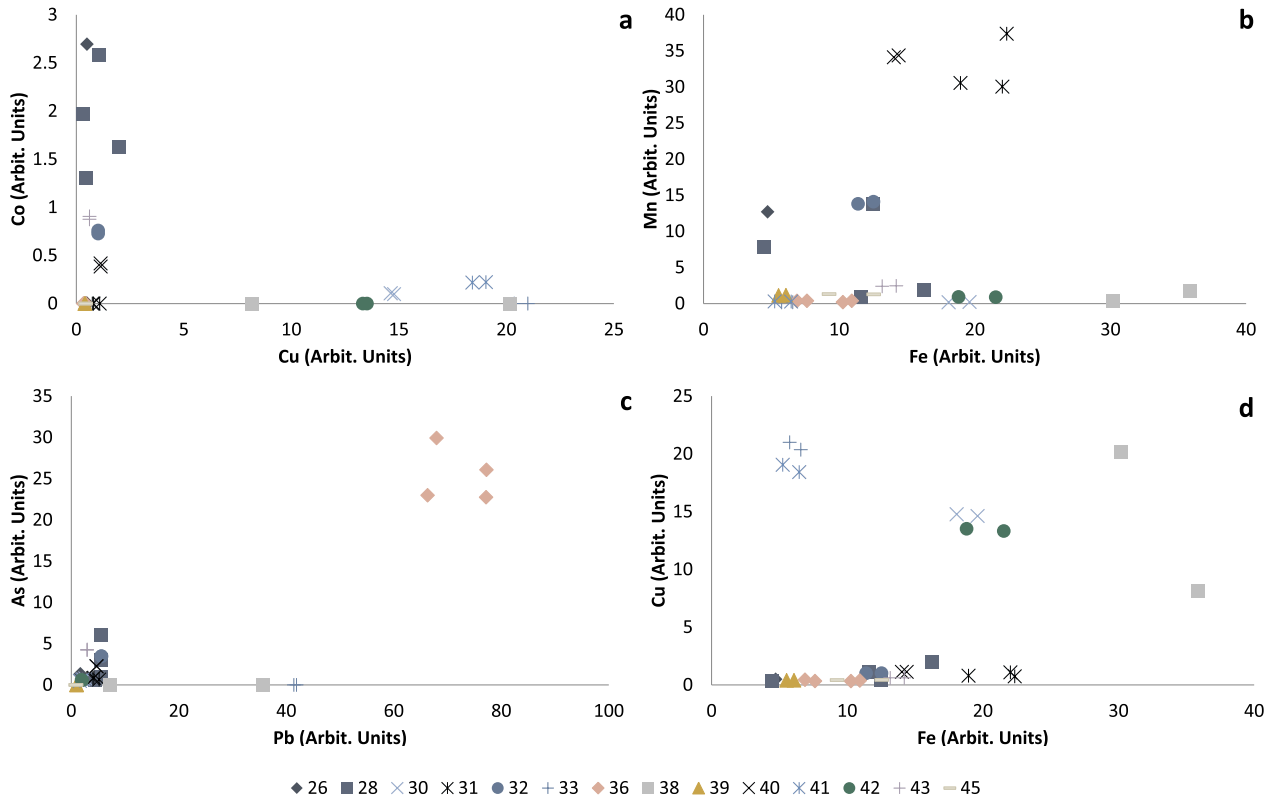

Fig. 3. a) hXRF Co-Cu plot indicating that the blue glass beads from types 26, 28, 32 and 43 are enriched in Co, while the blue glass beads from types 30, 33 and 41 are enriched in Cu; b) hXRF Mn-Fe plot corroborating the use of these two elements in the production of the black type 31 and 40 glass beads; c) hXRF Pb-As plot indicating that both Pb and As were used in the production of the glass beads from type 36; d) hXRF Cu-Fe plot substantiating the use of Cu and Fe to produce the green glass present in the type 38 and 42 glass beads.

Zn can be explained by the formation of sphalerite (ZnS), among other sulfides, in the final stages of the formation of five-element deposits [67]. Dayton [69] describes a sample composed of native silver, argentite (Ag_2S) and sphalerite recovered from the Schneeberg area, a known region of saffre[1] production since 1520. Chromium-rich minerals are also among the minerals found within the Erzgebirge mountain range. In fact, the type locality of magnesiochromite ($MgCr_2O_4$) is the Schwarzenberg area (Germany) [71].

Several inorganic compounds were identified in the blue glass beads using micro-Raman spectroscopy. Bands attributed to anatase – 143, 197, 396, 516, 637 cm^{-1} [72] – were identified in the type 43 glass beads, while a strong calcium phosphate band at 958 cm^{-1} [45] was found in the glass beads from type 28 indicating the that this compound was used to opacify these glass beads. Compounds that could derive from unmelted raw materials used in the glass production were found in the glass beads from types 30 and 33; the band at 996 cm^{-1} found in the type 30 glass beads was attributed to alkali sulfates such as glaserite ($((K_2)^{2+}(KNa)^{2+}(SO_4)_2{}^{4-})$ [73], while residual feldspar particles (518–519 cm^{-1} [73]) were found in the blue beads from type 33. The Raman spectra of the glass beads from types 26, 32 and 41 only revealed bands attributable to glass.

3.2.2. Black glass beads (types 31 and 40)

The hXRF results of the black beads classified as types 31 and 40 revealed significant amounts of Mn and Fe in their composition (Fig. 3b). The enrichment in both manganese and iron was further confirmed by VP-SEM-EDS (Table 2) and LA-ICP-MS (Table S2). Both hXRF and LA-ICP-MS also revealed minor amounts of Co (~ 442 ppm) in the type 40 glass beads. The combined use of metallic ions such as iron, manganese and cobalt has been used to produce black glass since the early stages of glass production [74].

A band at 143 cm^{-1} attributed to titanium dioxide [42] was identified by micro-Raman spectroscopy in the glass beads of type 40. While titanium compounds are known to have been used in the production of white glazes since the 19th century, these minerals are also among the most common impurities found in the raw materials used in glass production [75,76]. The ubiquitous nature of titanium oxides along with their large Raman cross section make these minerals easily detectably by micro-Raman spectroscopy even when present in very small quantities [75]. The Raman spectra of the glass beads from type 31 only revealed bands attributable to glass.

3.2.3. Red-on-white glass beads (type 36)

The hXRF and VP-SEM-EDS analysis of the red-on-white glass beads of type 36 did not allow the detection of any red-coloring elements. In this case, the use of LA-ICP-MS proved essential to determine the red colorant used in the manufacture of these glass beads. Trace amounts of gold (ca. 97 ppm) were introduced into the glass matrix in order to produce what is known as Cassius Purple or ruby red glass, as reported in European trade beads attributed to the Venetian production [77]. The process of dispersion of gold particles in glass was first described in Andreas Cassius' 1685 treatise [78].

Significant amounts of Pb and As were detected in the red-on-white beads by hXRF, VP-SEM-EDS (Table 2) and LA-ICP-MS (Table S2). In fact, the hXRF Pb-As plot (Fig. 3c) revealed a clear association between these two elements, which suggests that lead arsenates were used as the main opacifying agents. The use of this opacifier was further confirmed by micro-Raman spectroscopy; a band at 826–828 cm^{-1} attributed to

[1] A mixture of calcinated cobaltite (CoAsS) and smaltite ($(Co,Fe,Ni)As_2$) in siliceous sand used to produce cobalt-blue glass [2].

lead arsenates [16,45,75] was identified in both the red and white colored glass of the beads from type 36. Lead arsenates were first developed by the Venetian glass industry in the late 16th century [45,75], but were only broadly used since the 19th century [45]. Bands at 144 cm^{-1} and 983 cm^{-1} were also identified in the red glass by micro-Raman spectroscopy, and attributed to titanium dioxide [42] and α-wollastonite [75], respectively.

3.2.4. Amber glass beads (types 39 and 45)

As seen in Table 2, VP-SEM-EDS results showed that the type 39 and 45 amber colored glass beads are characterized by significant FeO and SO_2 concentrations, suggesting that the well-known iron-sulfur chromophore is responsible for their color. The iron-sulfur chromophore is produced when glasses are manufactured under strong reducing conditions and imparts an amber hue to the glass [48,79].

Micro-Raman spectroscopy only revealed bands attributable to glass.

The presence of opacifying agents was not determined by any analytical technique, which is consistent with the transparent nature of the type 39 and 45 glass beads.

3.2.5. Green glass beads (type 42)

The type 42 glass beads are characterized by significant Cu and Fe contents detectable by hXRF (Fig. 3d) and quantified by VP-SEM-EDS (Table 2) and LA-ICP-MS (Table S2). As previously mentioned, copper in its divalent state, imparts a turquoise hue to glass. Iron on the other hand can be used to produce blue, yellow or green depending on the Fe^{2+}/Fe^{3+} ratio present in the glass. The ferrous ions (Fe^{2+}) impart a blue hue to the glass, whereas the ferric ions (Fe^{3+}) gives it a pale-yellow tint, making the redox conditions used during the manufacture process essential to create the final glass color [56].

A band at 143 cm^{-1} attributed to titanium dioxide [42] was identified by micro-Raman spectroscopy. As previously mentioned, titanium oxides are commonly present as impurities in the raw materials used in glass production, and as they possess a large Raman cross section, are easily detectably by micro-Raman spectroscopy even when present in very small quantities [75].

3.2.6. Chevron glass bead with green, reddish-brown and white glass layers (type 38)

The chevron glass bead classified as type 38 consists of a surf green exterior glass layer, followed by consecutive layers of white, reddish brown and white glass and a gray glass core. The bulk composition of this glass bead was determined by hXRF, while the green, reddish-brown and white glass layers were analyzed by VP-SEM-EDS, LA-ICP-MS and micro-Raman spectroscopy.

The hXRF Cu-Fe plot (Fig. 3d) revealed that the type 38 glass bead was enriched in both copper and iron. In fact, both these transition metals are responsible for imparting green and reddish-brown colors to glass as confirmed by VP-SEM-EDS (Table 2) and LA-ICP-MS (Table S2). As previously mentioned, a combination of copper divalent ions and a green or yellow producing Fe^{2+}/Fe^{3+} ratio can impart a green hue to glass. This is most likely the case for the green glass of the type 38 beads. However, metallic copper (nano-)particles or cuprous oxide (Cu_2O) can be used to produce ruby-colored glass [2,7,55,78]. Studies have also found that low copper (CuO < 5 wt.%) and lead (10 < PbO < 10 wt.%) concentrations give rise to orange or brownish-red colored glass ([80] and references within). The red glass of the type 38 glass beads falls into this last category, having CuO and PbO concentrations of 1.0 and 7.8 wt.%, respectively. The addition of iron contributed to the final glass hue, darkening or lightening the brownish-red color according to the Fe^{2+}/Fe^{3+} ratio.

The white glass' color can be explained by the presence of high amounts of tin oxide (cassiterite) crystals as seen in Fig. 4. The enrichment in tin was also detected by hXRF and LA-ICP-MS.

3.3. Firing temperature

Micro-Raman spectroscopy is commonly used in the study of glass artefacts due to its versatility (e.g. [16,42,44,45,73,75,81]). The confocality and the micrometric spatial resolution of this technique allows not only the analysis of the glass matrix, but also the identification of the inorganic compounds responsible for the glass' color and opacity (e.g. [16,42,44,45,72,73,75,81]).

The Raman spectrum of silicate glass is characterized by the presence of two massifs corresponding to the bending and stretching modes of the Si-O bonds. The position of these massifs, centered at 500 and 1000 cm^{-1}, as well as their intensity is related to the glass' composition. First proposed by Colomban [81], the ratio between the areas of the bending and stretching massifs – known as polymerization index ($I_P = A_{500}/A_{1000}$) – is strongly correlated to the melting temperature of glass and to its composition [44,81]. The calculated I_P and their respective firing temperature can be found in Table 4.

These values are consistent with furnace temperatures achieved in European glass production centers (e.g. [82]), as well as firing temperatures of European trade beads previously reported by Rousaki et al. [83], Coccato et al. [84], and Costa et al. [16].

3.4. Glass sourcing

Determining the silica source is essential to establish the provenance of glass artefacts, as this raw material is usually found in the vicinity of the production site and not the subject of long-distance commercial trades such as the compounds used as fluxing or coloring agents. The ore sands used in glass production generally contain minor amounts of accessory minerals that are characteristic of the geological region from which the sand was obtained. The presence of these minerals within the silica source used in glass manufacture will be reflected in the composition of the glass artefacts produced and can be used as fingerprints of the different glass production centers.

Trace element and REE analysis has been used by many authors to successfully distinguish between different silica sources (e.g. [9–14,16–19,21–24]). The largest portion of REE found in glass can be attributed to the silica source, as these elements occur in insignificant concentrations in both plant ash and carbonates [24]. REE concentrations are also not influenced by the use of (de)colorants [14]. Moreover, while other trace elements can be influenced by erosion and sedimentation processes, REE preserve the signature of the source rock [22].

Costa et al. [16] established five compositional groups – groups A to E – based on the chondrite-normalized REE patterns of European trade beads found in the Church of Kulumbimbi (Mbanza Kongo, Angola). The authors also found a relationship between the REE patterns and the provenance of the glass beads: beads included in Groups A, D and E were most likely produced in Venice, while beads from Groups B and C were attributed to the Bohemian and the Bavarian glass industries, respectively. This relationship was established based on the probable origin initially assigned to each glass bead type by visual comparison with historic sample cards, museum collections, and archeological specimens, as well as the overall major and trace element composition of the glass beads. The determination of fluxing agents used in the production of the glass beads and the identification of opacifying agents used exclusively by certain production centers (e.g. the development of lead arsenates in the late 16th century by the Venetian glass industry) were particularly important to establish a credible link between provenance and chondrite-normalized REE patterns [16].

As seen in Fig. 5, these groups are essential to shed the light on the provenance of the glass beads found in Lumbu (Angola). The glass beads from types 30, 31, 36, 38, 41, 42 and 43 display REE patters similar to those of the previously defined Groups A and D (Fig. 5a), with an enrichment of light rare earth elements (LREE) relative to heavy rare earth elements (HREE; $(La/Yb)_{chondrite}$ = 6.57–10.05) and negative Eu

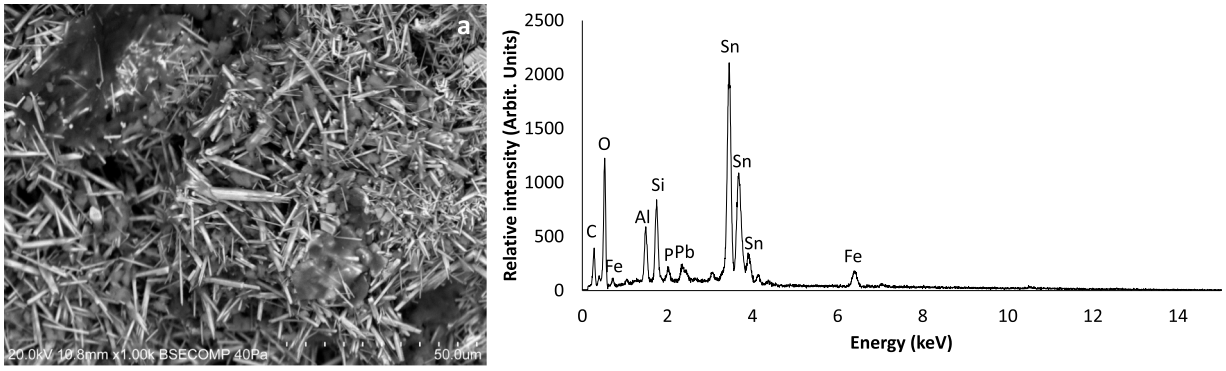

Fig. 4. a) VP-SEM image of the type 38 glass beads. The white areas were found to be tin oxide (cassiterite) crystals; b) point analysis of one of the cassiterite crystals.

Table 4
Polymerization index and corresponding firing temperature after Colomban [81]. The polymerization index was not calculated when significant inorganic phases were found to be superimposed on the glass Raman signature.

Glass bead type	Color	Polymerization index (I_P)	Estimated melting temperature (°C)
26	Dark blue	1.0	1000
28	Dark blue	0.9	1000
30	Blue	0.8	1000
31	Black	0.8	800–1000
32	Dark blue	1.1	1000
33	Blue	1.1	1000
36	Red		-
	White	1.0	1000
38	Green	1.0	1000
	Reddish-brown	0.8	800–1000
	White	0.7	800–1000
39	Amber	1.0	1000
40	Black	1.0	1000
41	Light blue	0.8	1000
42	Green	0.8	1000
43	Dark blue	1.1	1000
45	Amber	1.1	1000

anomalies (Eu/Eu* = 0.54–0.73) indicating a Venetian origin. The type 36 glass beads have the lowest absolute REE abundance, with can suggest that a purifying procedure was used to eliminate the minerals containing these elements from the sand (e.g. clays, monazite and zircon). However, it is important to note that the type 36 glass beads have significant Pb content, suggesting this element can be acting not only has an opacifier in the form of lead arsenates, but also as glass former and glass modifier, greatly diminishing the amount of sand used in glass production and therefore the REE introduced via the silica source.

The glass beads from types 39 and 45, on the other hand, have chondrite-normalized REE patterns characterized by Eu-anomalies close to 1 (Eu/Eu* = 0.84) and an enrichment in LREE when compared to the HREE ($(La/Yb)_{chondrite}$ = 6.97–7.07), which are comparable to those of Group E (Fig. 5b), indicating a Venetian origin.

The glass beads from types 32 and 40 display REE patters that are similar to those of Group D (Fig. 5c) with an enrichment of LREE relative to HREE ($(La/Yb)_{chondrite}$ = 5.51–7.32) and negative Eu anomalies (Eu/Eu* = 0.60–0.70). However, unlike the beads that compose Group D, the glass beads from types 32 and 40 have positive Ce anomalies (Ce/Ce* = 1.33–1.39). As these glass beads have significant amounts of MnO (Table 2; ca. 3.3 and 4.0 wt.%, respectively), the positive Ce-anomalies are most likely linked to the addition of pyrolusite (MnO_2) or psilomelane ($(BaH_2O)_2Mn_5O_{10}$) from hydrogenetic ferro-manganese crusts or nodules [85]. Based typological criteria and comparison with historic sample cards, museum collections, and archeological specimens, the type 40 glass beads are thought to have been manufactured in Venice (Table S1 – Supplementary information). Therefore, given their similar chemical signature, both the type 40 and the type 32 glass beads can be tentatively assigned to the Venetian glass industry.

The REE patterns of the glass beads from types 26 and 28 are characterized by a depletion of HREE when compared to LREE ($(La/Yb)_{chondrite}$ = 3.68–6.67) and significant negative Eu anomalies (Eu/Eu* = 0.28–0.43). The similarity between the REE patterns of these glass beads and those of Group B (Fig. 5d), suggests a Bohemian origin.

The REE pattern of the type 33 glass beads shows a very important enrichment in LREE in relation to HREE ($(La/Yb)_{chondrite}$ = 23.81) and negative Eu anomalies (Eu/Eu* = 0.58). This profile is similar to that of Groups A and D (Fig. 5c). However, a careful examination of the trace element concentrations shows distinct and important differences (Figs. 6 and 7). As seen in Fig. 6, the type 33 glass beads are enriched in Ta, when compared to the chondrite values and to the remaining glass beads that are similar to the previously defined Groups A and D. Tantalum is a rare transition element commonly found in association with niobium in minerals from the columbite-tantalite series [86]. Ta-bearing minerals are commonly found in pegmatites, granites and granite-related greisens, Ta-bearing cassiterite veins, and derived placers [87]. The type 33 glass beads also have significant amounts of K, Rb, Cs and Ba (Figs. 6 and 7). Rb^+, Cs^+ and Ba^+ have ionic radius similar to K^+, which allows these elements to be incorporated in the structure of K-bearing minerals such as phyllosilicates or K-feldspars [88]. These results are consistent with the use of sand deriving from granite-type rocks, with high amounts of heavy minerals. While these results do not exclude a Venice as the production area of the type 33 glass beads, they do not definitively prove this origin.

4. Conclusions

A multi-analytical minimally invasive methodology, which included handheld X-ray fluorescence (hXRF), variable pressure scanning electron microscope coupled with energy dispersive X-ray spectrometry (VP-SEM-EDS), micro-Raman spectroscopy and laser ablation inductively coupled plasma mass spectrometry (LA-ICP-MS), was used to study a collection of glass beads found in Lumbu (Mbanza Kongo, Angola). This combined multi-analytical approach permits bulk in situ analysis (hXRF), the determination of morphological aspects and the identification of inclusions (VP-SEM-EDS), the identification of the inorganic compounds responsible for the glass' color and opacity and the glass' firing temperature (micro-Raman spectroscopy) and trace element analysis (LA-ICP-MS).

The glass beads were initially subdivided based on typological criteria (Table S1 – Supplementary information). A probable origin was also assigned during this step by visual comparison with historic sample cards, museum collections, and archeological specimens.

Trace element analysis and rare earth element pattern analysis in

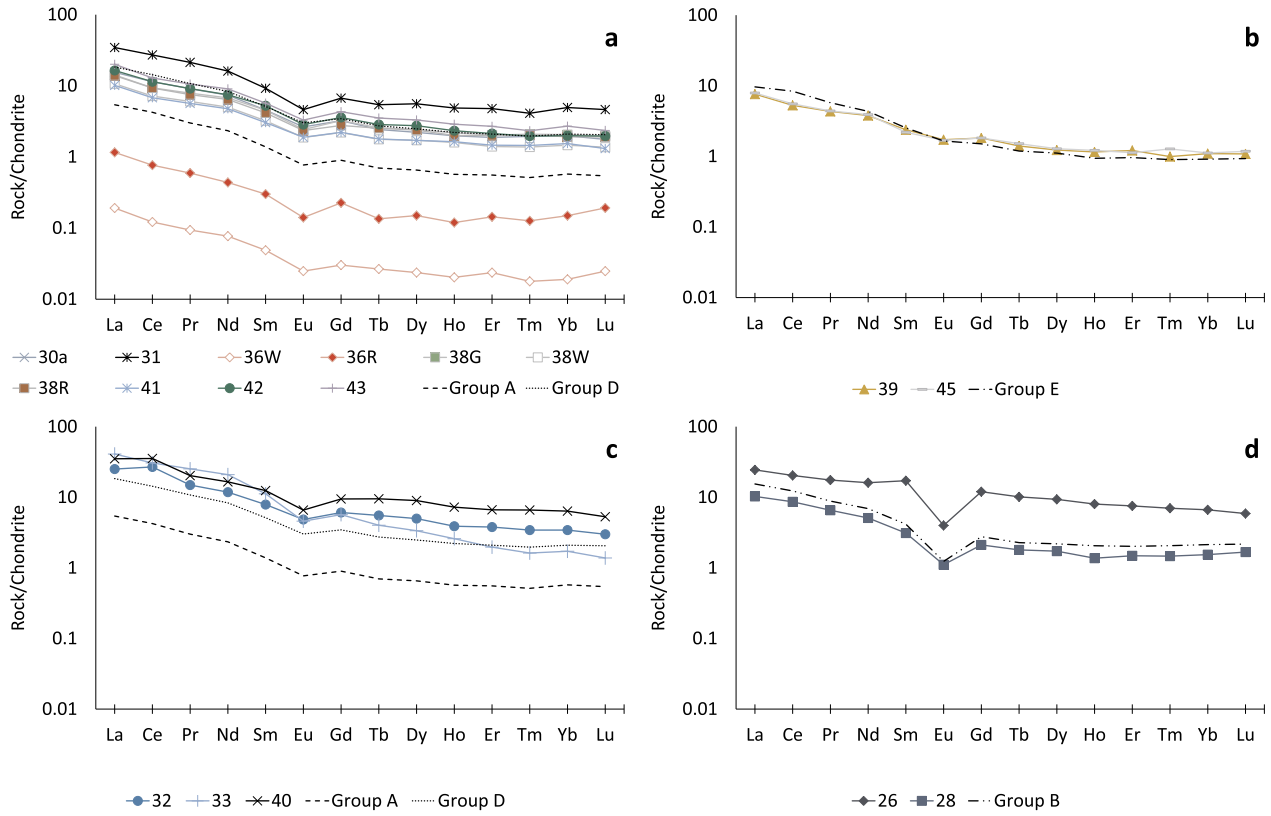

Fig. 5. Chondrite-normalized [89] REE patterns of the glass beads analyzed by LA-ICP-MS. Compositional groups A, B, D and E previously established by Costa et al. [16].

particular, was found to be essential to establish the provenance of the European trade beads in this study. Based on the compositional groups previously established by Costa et al. [16], the glass beads from types 30, 31, 32, 36, 38, 39, 40, 41, 42, 43 and 45 were found to have been produced in Venice, and the glass beads from types 26 and 28 have been assigned to the Bohemian glass industry.

While determining the provenance of each glass artefact was the main goal of this study, glass composition and the process of glass coloring and opacification were also studied in an attempt to establish the technology employed in the production of these artefacts. The determination of chemical glass type revealed the use of both *allume catina* and *barilla* or a combination of *allume catina* and *gripola di vino* to produce the Venetian glass beads, which is consistent with what is described in contemporaneous treaties. However, the glass beads manufactured in Bohemia were not produced using potash wood ash, presenting soda-lime or mixed alkali-lime composition. The estimated firing temperature of all glass beads was between 800 and 1000 °C.

Chemical data also indicate that cobalt and copper were used to produce blue hues, while a combination of copper and iron ions was used to produce green glass. Black colored glass was obtained by the combined use of iron and manganese ions, whereas the iron-sulfur chromophore was used to impart a distinct amber hue to the glass. Red

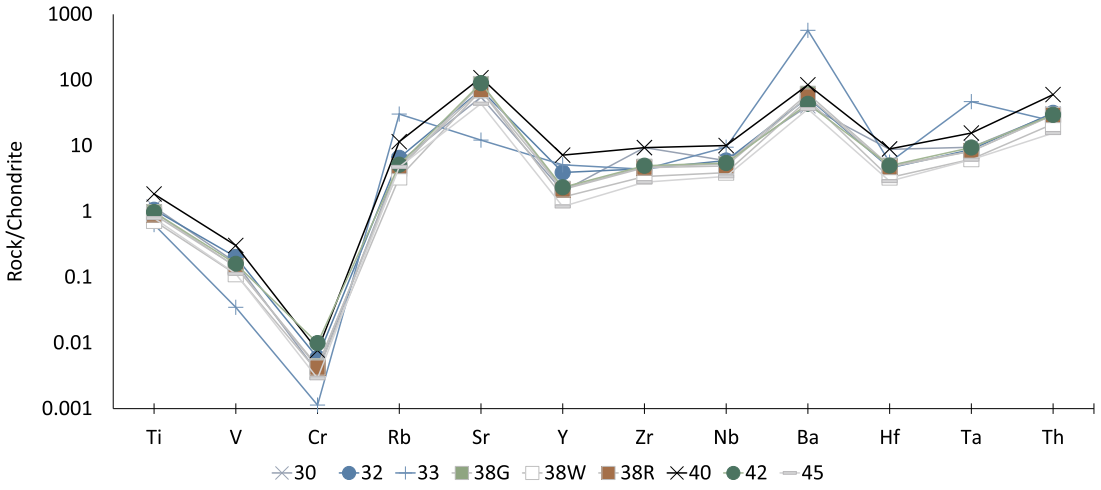

Fig. 6. Chondrite-normalized [89] trace element composition of a selection of glass beads found to have been produced in Venice (types 30, 32, 38, 40, 42 and 45) and the type 33 glass beads. The type 33 glass beads are enriched in Rb, Ba and Ta, when compared to the remaining beads displayed.

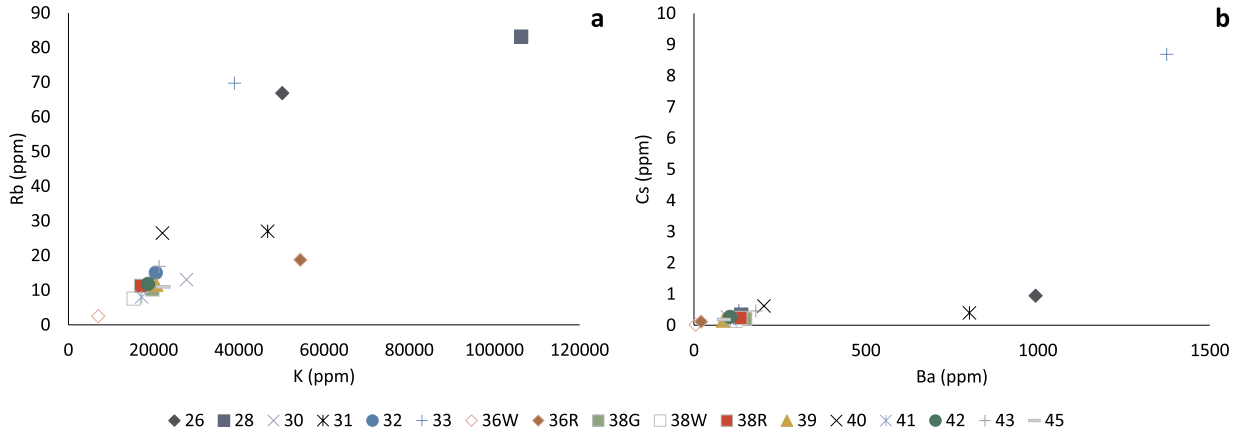

Fig. 7. Rb-K (a) and Cs-Ba (b) bi-plots evidencing the high K, Rb, Cs and Ba concentrations (obtained by LA-ICP-MS) present in the type 33 glass beads.

was produced using trace amounts of metallic gold particles (ruby red glass) and metallic copper nano-particles or cuprous oxide (brownish-red glass). Lead arsenates, calcium phosphate, and cassiterite were used as opacifying agents.

The use of both morphological and chemical analysis enabled the identification of distinct European production centers, allowing a glimpse into the consumption patterns and economic interactions in place between Europe and West-Central Africa throughout the 17th-19th centuries.

CRediT authorship contribution statement

Mafalda Costa: Conceptualization, Methodology, Validation, Formal analysis, Investigation, Writing - original draft, Visualization. **Pedro Barrulas:** Conceptualization, Methodology, Investigation, Validation. **Luís Dias:** Conceptualization, Investigation, Validation. **Maria da Conceição Lopes:** Conceptualization, Resources. **João Barreira:** Conceptualization, Resources. **Bernard Clist:** Conceptualization, Resources, Writing - review & editing. **Karlis Karklins:** Conceptualization, Methodology, Resources, Investigation, Writing - review & editing. **Maria da Piedade de Jesus:** Conceptualization, Resources, Project administration, Funding acquisition. **Sónia da Silva Domingos:** Conceptualization, Resources, Project administration, Funding acquisition. **Luc Moens:** Conceptualization, Resources. **Peter Vandenabeele:** Conceptualization, Methodology, Writing - review & editing, Funding acquisition. **José Mirão:** Conceptualization, Methodology, Validation, Investigation, Resources, Writing - review & editing, Supervision, Funding acquisition.

Declaration of Competing Interest

The authors declare that they have no known competing financial interests or personal relationships that could have appeared to influence the work reported in this paper.

Acknowledgments

The authors would like to thank the Angolan Governmentfor funding the archeological excavations carried out in the city of Mbanza Kongo during 2014, and the preliminary archeological laboratory work conducted in 2015, in the framework of the application for the recognition of Mbanza Kongo as part of the UNESCO World Heritage List. The authors would also like to thank the archeological excavation team headed by S. da Silva Domingos (CNIC, Angola), and Christophe Mbida and Raymond Assombang (University of Yaoundé I, Cameroon).

This work has also been financially supported by Fundação para a Ciência e para Tecnologia's(FCT) project UID/Multi/04449/2013 and by the European Regional Development Fund through the COMPETE 2020 project POCI-01-0145-FEDER-007649. M. Costa also acknowledges FCTfor a Ph.D. Fellowship (SFRH/BD/128889/2017) co-funded by the European Social Fund (ESF) and by Portuguese national funds.

The financial support provided by a Concerted Research Action (GOA) of Ghent University and by the Special Research Fund of Ghent University is also acknowledged.

Supplementary materials

Supplementary material associated with this article can be found, in the online version, at doi:10.1016/j.microc.2019.104531.

References

[1] Z. Goffer, Archaeological Chemistry, John Wiley & Sons, Hoboken, 2007.
[2] C. Moretti, S. Hreglich, Raw Materials, Recipes and procedures used for glass making, in: K. Janssens (Ed.), Mod. Methods Anal. Archaeol. Hist. Glas. I John Wiley & Sons, Ltd, 2013, pp. 23–47, , https://doi.org/10.1002/9781118314234.ch2.
[3] J. Henderson, The raw materials of early glass production, Oxford J. Archaeol. 4 (1985) 267–291, https://doi.org/10.1111/j.1468-0092.1985.tb00248.x.
[4] M.S. Tite, A.J. Shortland, Y. Maniatis, D. Kavoussanaki, S.A. Harris, The composition of the soda-rich and mixed alkali plant ashes used in the production of glass, J. Archaeol. Sci. 33 (2006) 1284–1292, https://doi.org/10.1016/j.jas.2006.01.004.
[5] S.C. Rasmussen, How Glass Changed the World: The History and Chemistry of Glass from Antiquity to the 13th Century, Springer, 2012.
[6] Z. Cílová, J. Woitsch, Potash - A key raw material of glass batch for Bohemian glasses from 14th-17th centuries? J. Archaeol. Sci. 39 (2012) 371–380, https://doi.org/10.1016/j.jas.2011.09.023.
[7] A.M. Pollard, C. Heron, Archaeological Chemistry, Second, The Royal Society of Chemistry, Cambridge, UK, 2008.
[8] I. Biron, M.-.H. Chopinet, Colouring, decolouring and opacifying of glass, in: K. Janssens (Ed.), Mod. Methods Anal. Archaeol. Hist. Glas. I John Wiley & Sons, Ltd, 2013, pp. 49–65.
[9] S.J. Saitowitz, Glass Beads as Indicators of Contact and Trade in Southern Africa ca. AD 900 - AD 1250, University of Cape Town, 1996.
[10] A. Aerts, B. Velde, K. Janssens, W. Dijkman, Change in silica sources in Roman and post-Roman glass, Spectrochim. Acta - Part B At. Spectrosc. 58 (2003) 659–667, https://doi.org/10.1016/S0584-8547(02)00287-2.
[11] K.H. Wedepohl, K. Simon, A. Kronz, The chemical composition including the rare earth elements of the three major glass types of Europe and the orient used in late antiquity and the middle ages, Chemie Der Erde - Geochemistry 71 (2011) 289–296, https://doi.org/10.1016/j.chemer.2011.04.001.
[12] M. Wood, S. Panighello, E.F. Orsega, P. Robertshaw, J.T. van Elteren, A. Crowther, M. Horton, N. Boivin, Zanzibar and Indian Ocean trade in the first millennium CE: the glass bead evidence, Archaeol. Anthropol. Sci. (2016) 1–23, https://doi.org/10.1007/s12520-015-0310-z.
[13] A. Blomme, P. Degryse, E. Dotsika, D. Ignatiadou, A. Longinelli, A. Silvestri, Provenance of polychrome and colourless 8th–4th century BC glass from Pieria, Greece: a chemical and isotopic approach, J. Archaeol. Sci. 78 (2017) 134–146, https://doi.org/10.1016/j.jas.2016.12.003.
[14] A. Ceglia, P. Cosyns, N. Schibille, W. Meulebroeck, Unravelling provenance and recycling of late antique glass with trace elements, Archaeol. Anthropol. Sci. (2017)

submitted.
[15] F. Bandama, S. Chirikure, S. Hall, C. Tinguely, Measly but motley and manifest: the typological and chemical characterisations of glass beads from the Southern Waterberg, Limpopo province of South Africa, J. Archaeol. Sci. Reports. 18 (2018) 90–99, https://doi.org/10.1016/j.jasrep.2017.12.047.
[16] M. Costa, P. Barrulas, L. Dias, M. da Conceição Lopes, J. Barreira, B. Clist, K. Karklins, M. da Piedade de Jesus, S. da Silva Domingos, P. Vandenabeele, J. Mirão, Multi-analytical approach to the study of the European glass beads found in the tombs of Kulumbimbi (Mbanza Kongo, Angola), Microchem. J. 149 (2019) 103990, , https://doi.org/10.1016/j.microc.2019.103990.
[17] P. Robertshaw, M.D. Glascock, M. Wood, R.S. Popelka, Chemical analysis of ancient African glass beads: a very preliminary report, J. African Archaeol 1 (2003) 139–146 http://www.jstor.org/stable/43134716.
[18] P. Robertshaw, B. Rasoarifetra, M. Wood, E. Melchiorre, R.S. Popelka-Filcoff, M.D. Glascock, Chemical analysis of glass beads from Madagascar, J. African Archaeol 4 (2006) 91–109.
[19] A.J. Shortland, N. Rogers, K. Eremin, Trace element discriminants between Egyptian and Mesopotamian late bronze age glasses, J. Archaeol. Sci. 34 (2007) 781–789, https://doi.org/10.1016/j.jas.2006.08.004.
[20] L. Dussubieux, C.M. Kusimba, V. Gogte, S.B. Kusimba, B. Gratuze, R. Oka, The trading of ancient glass beads: new analytical data from South Asian and East African soda-alumina glass beads, Archaeometry 50 (2008) 797–821, https://doi.org/10.1111/j.1475-4754.2007.00350.x.
[21] A. Silvestri, G. Molin, G. Salviulo, The coloured glass of Iulia Felix, J. Archaeol. Sci. 35 (2008) 331–341, https://doi.org/10.1016/j.jas.2007.03.010.
[22] P. Degryse, A.J. Shortland, Trace elements in provenancing raw materials for Roman glass production (An inaugural lecture to the society), Geol. Belgica. 12 (2009) 135–143 http://popups.ulg.ac.be/1374-8505/index.php?id=2723.
[23] P. Robertshaw, M. Wood, E. Melchiorre, R.S. Popelka-Filcoff, M.D. Glascock, Southern African glass beads: chemistry, glass sources and patterns of trade, J. Archaeol. Sci. 37 (2010) 1898–1912, https://doi.org/10.1016/j.jas.2010.02.016.
[24] K.H. Wedepohl, K. Simon, A. Kronz, Data on 61 chemical elements for the characterization of three major glass compositions in late antiquity and the middle ages, Archaeometry 53 (2011) 81–102, https://doi.org/10.1111/j.1475-4754.2010.00536.x.
[25] I.C. Freestone, Y. Gorin-Rosen, J.H. Michael, Primary glass from Israel and the production of glass in late antiquity and the early Islamic period, La Route Du Verre. Ateliers Primaires Second. Du Second Millénaire Avond J.C. Au Moyen Age. (2000) 65–84.
[26] S. Paynter, Analyses of colourless Roman glass from Binchester, county Durham, J. Archaeol. Sci. 33 (2006) 1037–1057, https://doi.org/10.1016/j.jas.2005.10.024.
[27] P. Degryse, R.B. Scott, D. Brems, The archaeometry of ancient glassmaking: reconstructing ancient technology and the trade of raw materials, Perspective (2014) 224–238, https://doi.org/10.4000/perspective.5617.
[28] J. Henderson, The provenance of ancient man-made glass: raw materials and the use of chemical and isotopic analytical techniques, in: I. Liritzis, C.M. Stevenson (Eds.), Obs. Anc. Manuf. Glas. University of New Mexico Press, 2012, pp. 185–201.
[29] D. Brems, P. Degryse, Trace element analysis in provenancing Roman glass-making, Archaeometry 56 (2014) 116–136, https://doi.org/10.1111/arcm.12063.
[30] C.R. DeCorse, F.G. Richard, I. Thiaw, Toward a systematic bead description system: a view from the lower Falemme, Senegal, J. African Archaeol 1 (2003) 77–109.
[31] K. Pallaver, ' A recognized currency in beads '. Glass beads as money in 19th-Century East Africa : the Central Caravan road, in: C. Eagleton, H. Fuller, J. Perkins (Eds.), Africa's Money in Africa, The British Museum, 2009, pp. 20–29.
[32] P. Robertshaw, S. Magnavita, M. Wood, E. Melchiorre, R. Popelka-Filcoff, M.D. Glascock, Glass beads from Kissi (Burkina Faso): chemical analysis and archaeological interpretation, J. African Archaeol. Monogr. Ser. 2 (2009) 105–118.
[33] L. Dussubieux, B. Gratuze, M. Blet-Lemarquand, Mineral soda alumina glass: occurence and meaning, J. Archaeol. Sci. 37 (2010) 1646–1655, https://doi.org/10.1016/j.jas.2010.01.025.
[34] M. Wood, A glass bead sequence for Southern Africa from the 8th to the 16th century AD, J. African Archaeol 9 (2011) 67–84.
[35] P. Robertshaw, M. Wood, A. Haour, K. Karklins, H. Neff, Chemical analysis, chronology, and context of a European glass bead assemblage from Garumele, Niger, J. Archaeol. Sci. 41 (2014) 591–604, https://doi.org/10.1016/j.jas.2013.08.023.
[36] F. Koleini, P. Colomban, I. Pikirayi, L.C. Prinsloo, G. Beads, Markers of ancient trade in Sub-Saharan Africa: methodology, state of the art and perspectives, Heritage 2 (2019) 2343–2369, https://doi.org/10.3390/heritage2030144.
[37] M.C. Lopes, Arquitectura e Arqueologia de Contacto na Valorização de Mbanza Kongo, a capital do Reino do Congo, Preservar o Património Português Além-Mar: Portugueses e a Salvaguarda do Património Edificado Português no Mundo, Caleidoscópio - Edição e Artes Gráficas, Casal de Cambra, SA, 2016, pp. 227–245.
[38] L. Heywood, Mbanza kongo / São Salvador: culture and the transformation of an African city 1491-1670s, in: E. Akyeampong, R.H. Bates, N. Nunn, J.A. Robinson (Eds.), Africa's Dev. Hist. Perspect. Cambridge University Press, Cambridge, UK, 2014, pp. 366–389.
[39] P. De Maret, Urban origins in central africa: the case of kongo, Dev. Urban. from a Glob. Perspect. Afrikansk och jämförande arkeologi, Uppsala, 2002, pp. 1–13.
[40] Z. Domingos, Preservação e Valorização do Património Arqueológico Angolano no Contexto Nacional e Mundial: caso do Sítio de Mbanza Kongo (Candidato a Património da Humanidade), Tecnol. E Ambient. 19 (2013) 262–275.
[41] M. Costa, A.M. Arruda, R. Barbosa, P. Barrulas, P. Vandenabeele, J. Mirão, A micro-analytical study of the scarabs of the necropolis of Vinha das Caliças (Portugal), Microsc. Microanal. 25 (2019) 214–220, https://doi.org/10.1017/S1431927618015600X.
[42] M. Costa, A.M. Arruda, L. Dias, R. Barbosa, J. Mirão, P. Vandenabeele, The combined use of Raman and micro-X-ray diffraction analysis in the study of archaeological glass beads, J. Raman Spectrosc 50 (2019) 250–261, https://doi.org/10.1002/jrs.5446.
[43] B.O. Mysen, L.W. Finger, D. Virgo, F.A. Seifert, Curve-fitting of Raman spectra of silicate glasses, Am. Mineral. 67 (1982) 686–695.
[44] P. Colomban, A. Tournié, L. Bellot-Gurlet, Raman identification of glassy silicates used in ceramics, glass and jewellery: a tentative, J. Raman Spectrosc 37 (2006) 841–852, https://doi.org/10.1002/jrs.1515.
[45] L.C. Prinsloo, A. Tournié, P. Colomban, A Raman spectroscopic study of glass trade beads excavated at Mapungubwe hill and K2, two archaeological sites in southern Africa, raises questions about the last occupation date of the hill, J. Archaeol. Sci. 38 (2011) 3264–3277, https://doi.org/10.1016/j.jas.2011.07.004.
[46] N.J.G. Pearce, W.T. Perkins, J.A. Westgate, M.P. Gorton, S.E. Jackson, C.R. Neal, S.P. Chenery, A compilation of new and published major and trace element data for NIST SRM 610 and NIST SRM 612 glass reference materials, Geostand. Newsl. – J. Geostand. Geoanalysis. 21 (1997) 115–144.
[47] O. Schalm, K. Janssens, H. Wouters, D. Caluwé, Composition of 12-18th century window glass in Belgium: non-figurative windows in secular buildings and stained-glass windows in religious buildings, Spectrochim. Acta - Part B At. Spectrosc. 62 (2007) 663–668, https://doi.org/10.1016/j.sab.2007.03.006.
[48] M. García-Heras, J.M. Rincón, A. Jimeno, M.A. Villegas, Pre-Roman coloured glass beads from the Iberian Peninsula: a chemico-physical characterisation study, J. Archaeol. Sci. 32 (2005) 727–738, https://doi.org/10.1016/j.jas.2004.12.007.
[49] L. Robinet, K. Eremin, Glass, in: H. Edwards, P. Vandenabeele (Eds.), Anal. Archaeom. Sel. Top. RSC Publishing, Cambridge, UK, 2012, pp. 268–290, , https://doi.org/10.1039/9781849732741.
[50] C.N. Duckworth, J. Henderson, F.J.M. Rutten, K. Nikita, Opacifiers in late bronze age glasses: the use of ToF-SIMS to identify raw ingredients and production techniques, J. Archaeol. Sci. 39 (2012) 2143–2152, https://doi.org/10.1016/j.jas.2012.02.011.
[51] B. Gratuze, K. Janssens, Provenance analysis of glass artefacts, in: K. Janssens, R. Van Grieken (Eds.), Compr. Anal. Chem. 1st ed., Elsevier Science, 2004, pp. 663–712, , https://doi.org/10.1016/S0166-526X(04)80019-9.
[52] I. Freestone, Teophilus and the composition of medieval glass.pdf, Mater. Res. Soc. 267 (1992) 739–745 https://doi.org/10.1557/PROC-267-739.
[53] K.H. Wedepohl, K. Simon, The chemical composition of medieval wood ash glass from Central Europe, Chemie Der Erde - Geochemistry 70 (2010) 89–97, https://doi.org/10.1016/j.chemer.2009.12.006.
[54] K. Janssens, S. Cagno, I. De Raedt, P. Degryse, Transfer of Glass Manufacturing Technology in the Sixteenth and Seventeenth Centuries from Southern to Northern Europe: Using Trace Element Patterns to Reveal the Spread from Venice via Antwerp to London, John Wiley & Sons, Ltd., 2013, https://doi.org/10.1002/9781118314234.ch25.
[55] P. Mirti, P. Davit, M. Gulmini, Colourants and opacifiers in seventh and eighth century glass investigated by spectroscopic techniques, Anal. Bioanal. Chem. 372 (2002) 221–229, https://doi.org/10.1007/s00216-001-1183-9.
[56] D. Möncke, M. Papageorgiou, A. Winterstein-Beckmann, N. Zacharias, Roman glasses coloured by dissolved transition metal ions: redox-reactions, optical spectroscopy and ligand field theory, J. Archaeol. Sci. 46 (2014) 23–36, https://doi.org/10.1016/j.jas.2014.03.007.
[57] T. Pradell, G. Molina, J. Molera, J. Pla, A. Labrador, The use of micro-XRD for the study of glaze color decorations, Appl. Phys. A Mater. Sci. Process. 111 (2013) 121–127, https://doi.org/10.1007/s00339-012-7445-x.
[58] D.G. Barceloux, Cobalt, Clin. Toxicol. 37 (1999) 201–2016, https://doi.org/10.1016/B978-0-12-386454-3.00832-0.
[59] G.V. Rao, Nickel and Cobalt Ores: Flotation, Encycl. Sep. Sci. Acad. Press, New York, 2000, pp. 3491–3500, https://doi.org/10.1016/B978-0-12-409547-2.10944-8.
[60] A. Zucchiatti, A. Bouquillon, I. Katona, A. D'Alessandro, The "della Robbia blue": a case study for the use of cobalt pigments in ceremics during the Italian Renaissance, Archaeometry 48 (2006) 131–152, https://doi.org/10.1111/j.1475-4754.2006.00247.x.
[61] T. Calligaro, PIXE in the study of archaeological and historical glass, X-Ray Spectrom 37 (2008) 169–177, https://doi.org/10.1002/xrs.1063 PIXE.
[62] J. Pérez-Arantegui, B. Montull, M. Resano, J.M. Ortega, Materials and technological evolution of ancient cobalt-blue-decorated ceramics: pigments and work patterns in tin-glazed objects from Aragon (Spain) from the 15th to the 18th century AD, J. Eur. Ceram. Soc. 29 (2009) 2499–2509, https://doi.org/10.1016/j.jeurceramsoc.2009.03.004.
[63] T. Seifert, D. Sandmann, Mineralogy and geochemistry of indium-bearing polymetallic vein-type deposits: implications for host minerals from the Freiberg district Eastern Erzgebirge, Germany, Ore Geol. Rev. 28 (2006) 1–31, https://doi.org/10.1016/j.oregeorev.2005.04.005.
[64] M. Scheinert, H. Kupsch, B. Bletz, Geochemical investigations of slags from the historical smelting in Freiberg, Erzgebirge (Germany), Chemie Der Erde 69 (2009) 81–90, https://doi.org/10.1016/j.chemer.2008.03.001.
[65] P. Ondrus, F. Veselovsky, A. Gabasova, J. Hlousek, V. Srein, Geology and hydrothermal vein system of the Jachymov (Joachimsthal) ore district, J. Czech Geol. Soc. 48 (2003) 3–18 http://www.jgeosci.org/index.php?pg=detail&ID=JCGS.946%5Cnhttp://www.jgeosci.org/content/JCGS2003_3-4_ondrus1.pdf.
[66] H.-J. Förster, R.L. Romer, B. Gottesmann, G. Tischendorf, D. Rhede, Are the granites of the Aue–Schwarzenberg Zone (Erzgebirge, Germany) a major source for metalliferous ore deposits? A geochemical, Sr–Nd–Pb isotopic, and geochronological study, Neues Jahrb. Für Mineral. - Abhandlungen. 186 (2009) 163–184, https://doi.org/10.1127/0077-7757/2009/0138.

[67] S.A. Kissin, Five-element (Ni-Co-As-Ag-Bi) veins, Geosci. Canada. 19 (1992) 113–124.
[68] J.R. Craig, D.J. Vaughan, Ore Microscopy and Ore Petrography, John Wiley & Sons, Inc., 1994.
[69] J.E. Dayton, Geological evidence for the discovery of cobalt blue glass in Mycenean times as a by-product of silver smelting in the Schneeberg area of the Bohemian Erzgebirge, Rev. d'archeometrie. 1 (1981) 57–61.
[70] E.S. Bastin, The nickel-cobalt-native silver ore type, Econ. Geol. 34 (1939) 1–40, https://doi.org/10.2113/gsecongeo.34.1.1.
[71] C. Biagioni, M. Pasero, Spinels Renaissance: the past, present, and future of those ubiquitous minerals and materials. The systematics of the spinel-type minerals: an overview, Am. Mineral. 99 (2014) 1254–1264.
[72] G.A. Tompsett, G.A. Bowmaker, R.P. Cooney, J.B. Metson, K.A. Rodgers, J.M. Seakins, The Raman spectrum of brookite, TiO2 (Pbca, Z = 8), J. Raman Spectrosc 26 (1995) 57–62, https://doi.org/10.1002/jrs.1250260110.
[73] P. Ricciardi, P. Colomban, A. Tournié, M. Macchiarola, N. Ayed, A non-invasive study of Roman age mosaic glass tesserae by means of Raman spectroscopy, J. Archaeol. Sci. 36 (2009) 2551–2559, https://doi.org/10.1016/j.jas.2009.07.008.
[74] B. Velde, Glass compositions over several millennia in the Western World, in: K. Janssens (Ed.), Mod. Methods Anal. Archaeol. Hist. Glas. I John Wiley & Sons, Ltd, 2013, pp. 67–78.
[75] P. Ricciardi, P. Colomban, A. Tournie, V. Milande, Nondestructive on-site identification of ancient glasses: genuine artefacts, embellished pieces or forgeries? J. Raman Spectrosc 40 (2009) 604–617, https://doi.org/10.1002/jrs.2165.
[76] S. Teixeira, A.M. Bernardin, Development of TiO2 white glazes for ceramic tiles, Dye. Pigment. 80 (2009) 292–296, https://doi.org/10.1016/j.dyepig.2008.07.017.
[77] L.E. Burgess, L. Dussubieux, Chemical composition of late 18th- and 19th-century glass beads from western North America: clues to sourcing beads, BEADS J. Soc. Bead Res. (2007) 58–73.
[78] P. Colomban, The use of metal nanoparticles to produce yellow, red and iridescent colour, from bronze age to present times in lustre pottery and glass: solid state chemistry, spectroscopy and nanostructure, J. Nano Res. 8 (2009) 109–132, https://doi.org/10.4028/www.scientific.net/JNanoR.8.109.
[79] J.W.H. Schreurs, R.H. Brill, Iron and sulfur related colors in ancient glasses, Archaeometry 26 (1984) 199–209.
[80] A. Silvestri, S. Tonietto, G. Molin, P. Guerriero, The palaeo-Christian glass mosaic of St. Prosdocimus (Padova, Italy): archaeometric characterisation of tesserae with copper- or tin-based opacifiers, J. Archaeol. Sci. 42 (2014) 51–67, https://doi.org/10.1016/j.jas.2013.10.018.
[81] P. Colomban, Polymerization degree and raman identification of ancient glasses used for jewelry, ceramic enamels and mosaics, J. Non. Cryst. Solids. 323 (2003) 180–187, https://doi.org/10.1016/S0022-3093(03)00303-X.
[82] W.P. McCray, The Culture and Technology of Glass in Renaissance Venice, University of Arizona, 1996.
[83] A. Rousaki, A. Coccato, C. Verhaeghe, B. Clist, K. Bostoen, P. Vandenabeele, L. Moens, Combined spectroscopic analysis of beads from the Tombs of Kindoki, lower Congo Province (Democratic Republic of the Congo), Appl. Spectrosc. 70 (2016) 79–93, https://doi.org/10.1177/0003702815616595.
[84] A. Coccato, M. Costa, A. Rousaki, B.-.O. Clist, K. Karklins, K. Bostoen, A. Manhita, A. Cardoso, C. Barrocas Dias, A. Candeias, L. Moens, J. Mirão, P. Vandenabeele, Micro-Raman spectroscopy and complementary techniques (hXRF, VP-SEM-EDS, μ-FTIR and Py-GC/Ms) applied to the study of beads from the Kongo Kingdom (Democratic Republic of the Congo), J. Raman Spectrosc 48 (2017) 1468–1478, https://doi.org/10.1002/jrs.5106.
[85] M. Bau, K. Schmidt, A. Koschinsky, J. Hein, T. Kuhn, A. Usui, Discriminating between different genetic types of marine ferro-manganese crusts and nodules based on rare earth elements and yttrium, Chem. Geol. 381 (2014) 1–9, https://doi.org/10.1016/j.chemgeo.2014.05.004.
[86] W. Köck, P. Paschen, Tantalum-processing, properties and applications, Jom 41 (1989) 33–39, https://doi.org/10.1007/BF03220360.
[87] P. Cerny, Characteristics of pegmatite deposits of tantalum, Lanthanides, Tantalum and Niobium (1989) 195–239.
[88] D.G. Brookins, Geochemical Aspects of Radioactive Waste Disposal, Springer-Verlag, New York, 1984, https://doi.org/10.1007/978-1-4613-8254-6.
[89] W.F. McDonough, S.-s. Sun, The composition of the Earth, Chem. Geol. (Isotope Geosci. Sect. 120 (1995) 223–253.